

SPOTLIGHT

How micron-sized exocrine vesicles release content: A comparison with sub-micron endocrine vesicles

Lisi Wei¹, Xin Wang¹, and Ling-Gang Wu¹

Exocytosis releases vesicular contents to mediate physiological functions. In this issue, Biton et al. (<https://doi.org/10.1083/jcb.202302112>) found four modes of releasing micron-sized exocrine vesicles and the underlying mechanisms involving actomyosin and BAR domain proteins. We highlight their discovery, compare it with much smaller/faster neuroendocrine vesicle fusion, and draw distinct and conserved principles regarding their membrane transformations, pore dynamics, and underlying mechanisms.

Exocytosis releases vesicular contents, including transmitters, hormones, and peptides, to mediate diverse functions, such as synaptic transmission essential for brain functions, stress responses, blood glucose levels critical for diabetes, and immune responses (1, 2). Vesicle fusion at the plasma membrane generates an Ω -shaped profile with a fusion pore that may expand, constrict, and/or close, while the Ω profile may enlarge, shrink, or merge at the plasma membrane. By super-resolution imaging of the fluorescently labeled membrane and vesicular contents, these vesicular fusion membrane transformations have been directly observed and shown to critically control content release in neuroendocrine chromaffin cells containing ~ 300 nm vesicles, which release contents within milliseconds to seconds (3–6). Would these membrane transformations and underlying mechanisms be conserved among different vesicle sizes ranging from ~ 30 to 60 nm synaptic vesicles that release neurotransmitters in milliseconds to ~ 2 – 10 μ m large secretory vesicles (LSV) in exocrine cells that release viscous contents in minutes? In this issue, Biton et al. (7) report fusing LSV membrane transformation and underlying mechanisms in *Drosophila* larval salivary glands, which release adhesive

mucinous glycoproteins nicknamed “glue” to facilitate metamorphosis.

The large size and slow release of LSV allow for real-time viewing of membrane transformations with confocal microscopy (8–12) and resolution-improved image processing (7). By imaging fluorescently labeled LSV lumen protein (e.g., Sgs3-GFP) and fusing-LSV-surrounding F-actin (e.g., Life-Act-Ruby), recent studies revealed a fusion mode termed membrane crumpling—the actomyosin-generated contraction that shrinks the fusion-generated Ω profile partially, folds Ω profile membrane, and squeezes out glue (Fig. 1 A) (8–12). Building on these studies, Biton et al. (7) dissected the fusion pore dynamics and underlying mechanisms that may generate other fusion modes besides membrane crumpling.

The authors reported three additional modes: (1) full-collapse-like, involving Ω profile shrinking until its width is smaller than the pore, after which the Ω profile is converted to a Δ -shaped profile and then flat membrane; (2) kiss-and-run, involving Ω profile pore closure, and (3) stalling, involving Ω profile staying unchanged (Fig. 1 A) (7). Detection of kiss-and-run or stalling seems difficult, as it was not possible to unambiguously determine whether the vesicle is before or after fusion or with an

opened or closed pore in some exampled fluorescent images of vesicular contents and F-actin. Verifying these modes with additional methods in the future would be beneficial.

Biton et al. (7) found that knockdown or pharmacological inhibition of actin-related protein 2/3 (Arp2/3), a branched actin polymerization nucleator, reduced membrane crumpling but enhanced kiss-and-run that used a narrower pore, suggesting F-actin involvement in pore expansion. Similarly, pharmacological inhibition or genetic manipulation of Bin-Amphiphysin-Rvs (BAR) domain proteins involved in F-actin assembly, including Cdc42-interacting protein 4 (CIP4) and Missing-in-Metastasis (MIM), reduced membrane crumpling but enhanced kiss-and-run, suggesting their involvement in pore expansion (7). Pharmacological inhibition or knockdown of myosin II slows down fusion pore expansion, suggesting myosin II involvement in pore expansion. Thus, F-actin, Arp2/3, CIP4, and MIM are involved in pore expansion (Fig. 1 C).

Knockdown of Arp3, MIM, or another BAR domain protein sorting nexin 1 that may sense membrane curvature enhanced full-collapse-like fusion, suggesting their involvement in pore stabilization. Pharmacological inhibition or knockdown of

¹National Institute of Neurological Disorders and Stroke, Bethesda, MD, USA.

Correspondence to Ling-Gang Wu: wul@ninds.nih.gov; Lisi Wei: lisi.wei@nih.gov.

This is a work of the U.S. Government and is not subject to copyright protection in the United States. Foreign copyrights may apply. This article is distributed under the terms of an Attribution–Noncommercial–Share Alike–No Mirror Sites license for the first six months after the publication date (see <http://www.rupress.org/terms/>). After six months it is available under a Creative Commons License (Attribution–Noncommercial–Share Alike 4.0 International license, as described at <https://creativecommons.org/licenses/by-nc-sa/4.0/>).

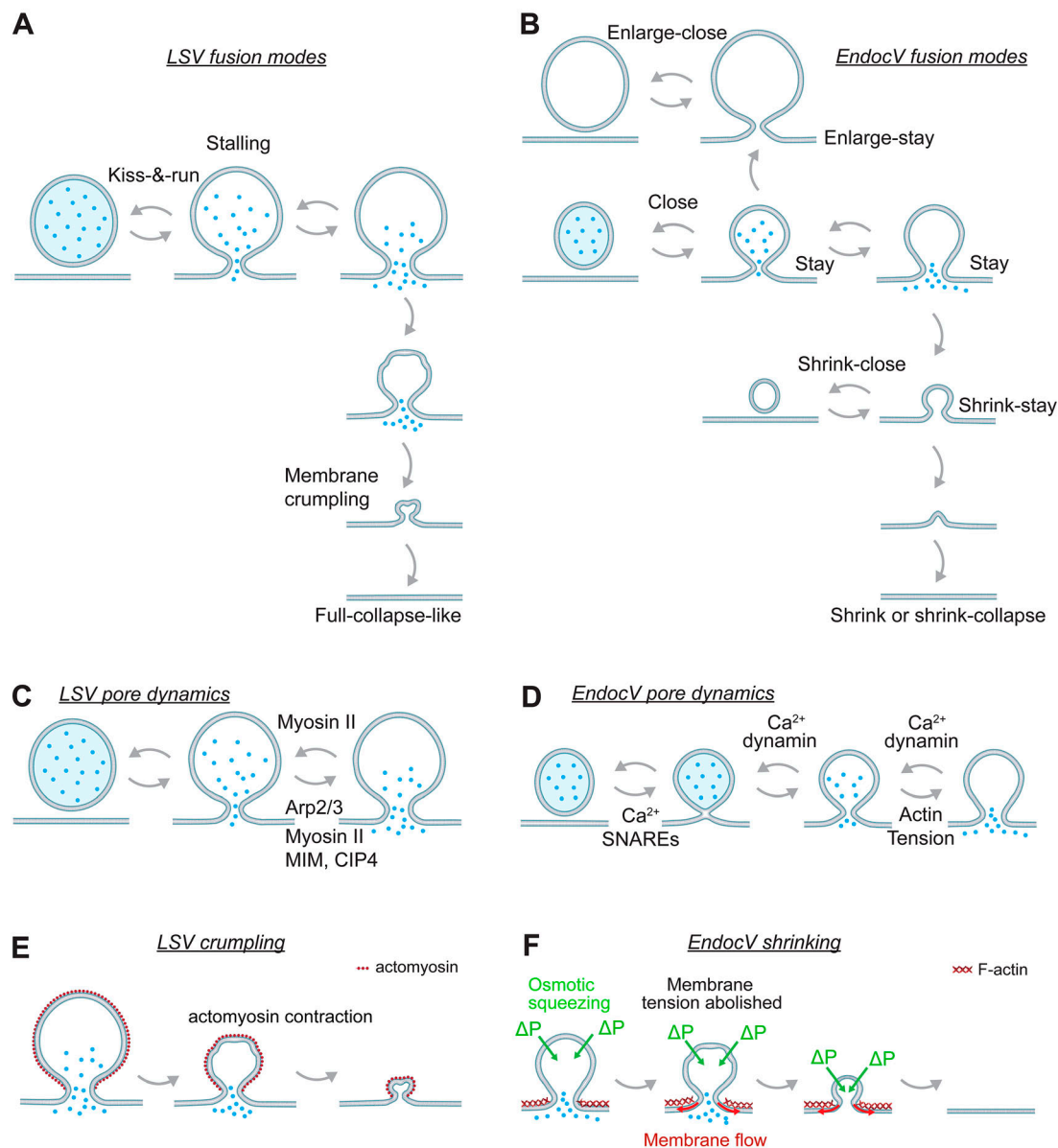


Figure 1. Comparison of the fusion membrane dynamics between large exocrine vesicles and smaller endocrine vesicles. (A and B) Fusion modes regarding Ω profile membrane size/shape changes and pore status in LSV of exocrine cells (A) and smaller endocrine vesicles (EndocV) in chromaffin cells (B). Note that different naming systems used in A and B may refer to the same fusion mode. **(C and D)** LSV (C) and EndocV (D) pore dynamics: competition between fusion pore expansion and constriction mechanisms determines the fusion pore dynamics, including expansion, constriction, and closure. A hemi-fusion structure is included in D because it is detectable during EndocV fusion and dynamin may antagonize hemi-to-full fusion. **(E and F)** Mechanisms underlying Ω profile shrinking and membrane crumpling for LSV (E) and EndocV fusion (F). ΔP , a positive osmotic pressure difference between intra- and extracellular solution; membrane flow, F-actin-supported tension at the plasma membrane reels in the low-tension Ω profile membrane, resulting in the shrinking of the Ω profile.

myosin II slowed or blocked pore constriction, suggesting myosin II involvement in pore constriction (Fig. 1 C). Thus, actomyosin and BAR domain proteins cooperate to expand the pore initially and subsequently stabilize and constrict the pore (Fig. 1 C) (7).

Are these LSV membrane transformations and underlying mechanisms applicable to smaller vesicles? Ω profiles generated from ~300 nm vesicle fusion in neuroendocrine

chromaffin cells may (1) remain unchanged (stay fusion), (2) close their pore within milliseconds to tens of seconds regardless of the pore size (close fusion), (3) shrink partially (shrink-stay fusion), (4) shrink partially, followed by pore closure (shrink-close), (5) shrink until its size is smaller than its pore, after which the Ω profile is converted to Λ - and then flat-shaped, termed shrink or shrink-collapse fusion, (6)

enlarge (enlarge-stay), or (7) enlarge, followed by pore closure (enlarge-close, Fig. 1 B) (3, 5, 6). Surprisingly, classical full-collapse fusion involving no shrinking but pore dilation until flattening has not been observed.

LSV's full-collapse-like fusion, kiss-and-run, and stalling are morphologically reminiscent of neuroendocrine vesicle's shrink-collapse, close, and stay fusion,

respectively, except that close or stay fusion may involve either a small pore to restrict release or a large pore to promote release. LSV's membrane crumpling mode is analogous to shrink-stay, except Ω profile membrane crumpling. We, therefore, suggest using a unifying naming system in Fig. 1 B to describe fusion modes with different Ω profile size and pore dynamics: "shrink" refers to Ω profile shrinking; "shrink-collapse," Ω profile shrinking first followed by pore dilation; "close," pore closure; "stay," Ω profile staying at the plasma membrane. We suggest using "shrink-stay-crumple" to indicate membrane crumpling, which may more visually describe it and its conversion to shrink-collapse (full-collapse-like, Fig. 1 A). This naming system may accommodate additional modes yet to be found for any vesicle, such as pore closure after shrink-stay-crumple.

In neuroendocrine cells, competition between pore expansion and constriction determines fusion pore dynamics (Fig. 1 D) (4, 5). The constriction mechanism, mediated by pore-surrounding dynamin scaffolds, may compete with the pore opening mechanism at the hemi-fusion stage to prevent hemi-to-full fusion (Fig. 1 D) (4) and at the full-fusion instant to decide the initial pore size and release kinetics (Fig. 1 D) (5). This competition principle seems conserved for LSV but with two distinct features (Fig. 1 C). First, myosin II-mediated constriction acts at a much later stage, tens to hundreds of seconds after the fusion onset, to counteract LSV pore expansion (7). In contrast, pharmacological inhibition of myosin II broadens the

amperometric spike half-width in endocrine cells, implying that myosin II facilitates endocrine vesicle pore expansion (13). Second, F-actin, Arp2/3, CIP4, and MIM are involved in expanding LSV pore via an as-yet-unidentified force-generation mechanism (7). In contrast, cortical F-actin provides tension at the plasma membrane to expand the endocrine vesicle fusion pore (6, 14). These results raise the possibility that F-actin, Arp2/3, CIP4, and MIM might provide plasma membrane tension for pore expansion of both LSV and endocrine vesicles.

Shrink-stay and shrink-stay-crumple are similar in shrinking and F-actin involvement but different in driving forces. In endocrine cells, a positive osmotic pressure difference between intra- and extracellular solution squeezes the Ω profile and reduces its membrane tension, which might, in principle, also fold the membrane (Fig. 1 F) (6). However, the higher tension at the plasma membrane supported by F-actin reels off the low-tension Ω profile membrane, shrinking the Ω profile in seconds or less (Fig. 1 F) (6). Upon exocrine vesicle fusion, actomyosin assembles around and contracts the fusing Ω profile to shrink the Ω profile and fold its membrane in minutes (Fig. 1 E) (8–10). Some LSV shrink-stay-crumple (membrane crumpling) events can be converted to shrink-collapse (full-collapse-like) (7). F-actin-dependent plasma membrane tension might reel off the low-tension, crumpled LSV Ω profile membrane as in endocrine cells, resulting in LSV shrink-collapse fusion.

In summary, actomyosin and BAR domain protein assembly around the fusing Ω

profile may control Ω profile size, pore dynamics, and thus, the release time of LSV. The basic principles governing LSV membrane transformations and underlying mechanisms are analogous to smaller neuroendocrine vesicles to a large extent but with a unique feature—the actomyosin-mediated Ω profile shrinking with membrane crumpling, likely due to the physiological demand of releasing sticky contents from micrometer-sized vesicles. Understanding LSV fusion may thus also shed light beyond LSV to smaller vesicles.

References

1. Wu, L.G., et al. 2014. *Annu. Rev. Physiol.* <https://doi.org/10.1146/annurev-physiol-021113-170305>
2. Sharma, S., and M. Lindau. 2018. *FEBS Lett.* <https://doi.org/10.1002/1873-3468.13160>
3. Chiang, H.C., et al. 2014. *Nat. Commun.* <https://doi.org/10.1038/ncomms4356>
4. Zhao, W.D., et al. 2016. *Nature*. <https://doi.org/10.1038/nature18598>
5. Shin, W., et al. 2018. *Cell*. <https://doi.org/10.1016/j.cell.2018.02.062>
6. Shin, W., et al. 2020. *Cell Rep.* <https://doi.org/10.1016/j.celrep.2019.12.044>
7. Biton, T., et al. 2023. *J. Cell Biol.* <https://doi.org/10.1083/jcb.202302112>
8. Rouso, T., et al. 2016. *Nat. Cell Biol.* <https://doi.org/10.1038/ncb3288>
9. Kamlesh, K., et al. 2021. *Dev. Cell*. <https://doi.org/10.1016/j.devcel.2021.05.004>
10. Tran, D.T., et al. 2015. *Nat. Commun.* <https://doi.org/10.1038/ncomms10098>
11. Nightingale, T.D., et al. 2011. *J. Cell Biol.* <https://doi.org/10.1083/jcb.201011119>
12. Nightingale, T.D., et al. 2012. *Trends Cell Biol.* <https://doi.org/10.1016/j.tcb.2012.03.003>
13. Berberian, K., et al. 2009. *J. Neurosci.* <https://doi.org/10.1523/JNEUROSCI.2818-08.2009>
14. Wen, P.J., et al. 2016. *Nat. Commun.* <https://doi.org/10.1038/ncomms12604>